J. Membrane Biol. 11, 197–216 (1973)

The Teorell Membrane Oscillator as a Mechano-Electric Transducer

P. Meares and K. R. Page

Biophysical Chemistry Unit, Department of Chemistry, University of Aberdeen, Old Aberdeen, Scotland

Received 3 July 1972

Summary. The results of a recent quantitative analysis of the Teorell membrane oscillator are utilized to explore its role as an excitability analogue. Special attention is paid to its role as a mechano-electric transducer. A membrane of exceptionally well-defined pore structure has been used in this study. The analogue properties arise from nonlinear coupling between water and salt fluxes. When the membrane is simultaneously subjected to controlled gradients of hydrostatic pressure, electrical potential and concentration, bi-stable stationary states can be produced. These arise from the opposing effects of pressure and electro-osmosis on the volume flow. Transitions between these states show hysteresis. The factors governing such transitions are analogous to certain types of stimuli encountered in the natural excitation process. The membrane system also shows oscillatory behavior when the hydrostatic pressure gradient is allowed to vary under constant current conditions. This property is related to the bi-stable stationary state phenomena and is compared to the regenerative behavior found in biologically excitable tissues. Particular emphasis is placed upon analogies between the membrane oscillator and certain natural tissues. The importance of the nonlinear nature of the force-flux coupling in the analogue is stressed, and its possible relevance to biological excitability indicated. Some consideration is also given to the role of electro-osmotic flux coupling in biological tissues.

The Teorell membrane oscillator consists of a broad-pored membrane of low effective internal electric charge separating concentrated and dilute solutions of the same electrolyte. The passage of an appropriate electric current through the membrane gives rise to an electro-osmotic flux directed from the dilute to the concentrated solution. This is opposed by a hydrodynamic flow induced by pressure applied across the membrane.

This membrane system may exist in either one of two stable states depending on the magnitudes of the membrane potential and the applied pressure differential. The occurrence of transitions between these states for a given inelastic membrane and pair of solutions is a function only of potential, pressure and temperature. Thus, pressure impulses can be turned

into electric events and vice versa, and regenerative phenomena can occur (Drouin, 1969). As will be shown later, similar transitions can be predicted to occur when an elastic membrane is stretched. This membrane system can therefore provide an interesting analogue of biological mechano-electric transduction such as is encountered in natural pressure-sensitive receptors (Teorell, 1966; Loewenstein, 1971).

Until recently, the use of the Teorell oscillator as an analogue has been hampered by the absence of a sufficiently detailed understanding of its operation. Previous work had been confined to sinter and compressed powder membranes (Teorell, 1959*a*; Jancke, 1962; Franck, 1963; Drouin, 1969). Composite membranes have irregular pore structures that are difficult to analyze and theoretical treatments of such composites have required assumptions about the uniformity and homogeneity of pore charge that are not suited to heterogeneous structures (Teorell, 1959*b*; Franck, 1963).

Recently, Meares and Page (1972) have re-examined the Teorell oscillator using a membrane with well-defined parallel pores. This has facilitated the theoretical analysis of the system and permitted a quantitative comparison between theory and experiment. It has been found that an approach along the lines laid down by Kobatake and Fujita (1964) and by Mikulecky and Caplan (1966) successfully describes the stationary-state properties of the oscillator. These give rise to the so-called "flip-flop" phenomena. The purpose of this paper is to apply the results of that study of stationary states and transitions to the interpretation of the mechano-electric transducer properties of the Teorell oscillator.

The Flip-Flop Phenomena

The flip-flop phenomena are observed using the apparatus shown in Fig. 1. The membrane M separates the solutions in compartments I and II. The membrane potential $\Delta\psi_T$ is sensed by probe electrodes connected to the cell interior through the salt bridges B. A constant current is passed through the membrane via the electrodes E. Constant level reservoirs X permit various pressure differentials ΔP to be applied across the membrane. Compartment I is filled with dilute and compartment II with concentrated electrolyte. Each is stirred by paddles and electrolyte is continuously circulated between the compartment and an enclosed reservoir of 1-liter capacity. The whole cell is placed in an air thermostat maintained at 25 °C.

Fig. 2 illustrates a characteristic current *vs.* potential plot showing flip-flop behavior obtained using this apparatus. At low currents the volume flow is controlled by the pressure differential and flows from the concentrated

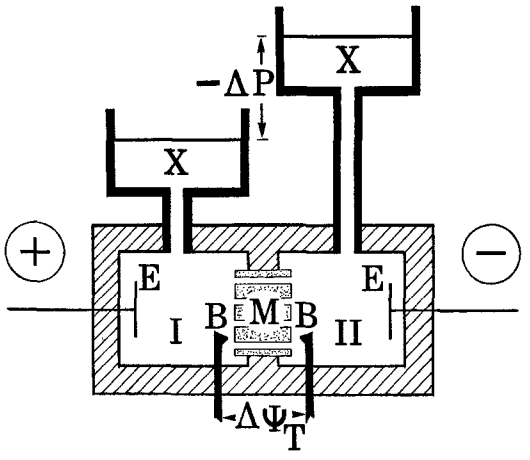

Fig. 1. Membrane apparatus used for studying stationary states

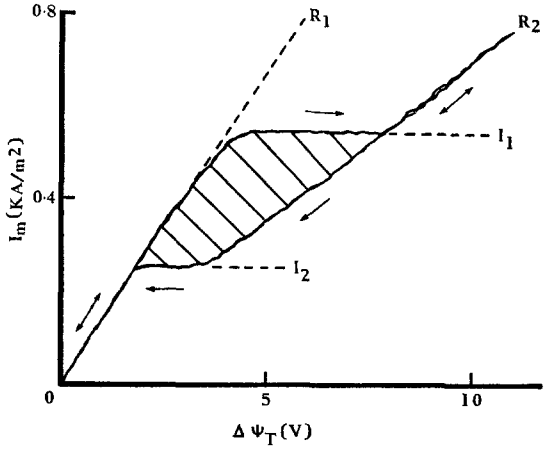

Fig. 2. Galvanostatic current density *vs.* total potential difference. The trace was obtained using a pressure clamp of −589 Pa across 13 mm^2 of membrane A. The membrane separated solutions of 0.1 and 0.01 mol dm^{-3} NaCl

to the dilute solution. The electrical resistance of the membrane is consequently low because it is filled with the more-concentrated solution. At a critical current density I_1 flip-over occurs because the effect of electro-osmosis overcomes the pressure-driven flow. The volume flux now reverses direction, the membrane fills with the dilute solution and its resistance rises. On decreasing the current density a second transition point I_2 is encountered and the reverse sequence of events occurs. I_2 is called the flop-over current and is lower than I_1. The pressure difference ΔP, the resistances R_1 and R_2 and the currents I_1 and I_2 characterize this cycle for a given membrane and pair of electrolyte concentrations.

The Membrane

General Electric Nuclepore filters were found suitable for the exact study of these phenomena. They consist of a thin sheet of polycarbonate perforated by a nearly parallel array of right circular pores. A negative charge is associated with the polycarbonate surface and electro-osmotic flow in the pores occurs in the direction of the cation flux. The membranes are supplied in a series of graded pore sizes and densities; i.e., number of pores per unit area.

Because the membranes were thin and of high permeability it was necessary to take into account stagnant layers of solution adjacent to the membrane. The method of doing this together with other experimental details have been published elsewhere (Meares & Page, 1972).

Theoretical

The parallel pored structure of a Nuclepore membrane permits an analysis of its behavior to be given in terms of that of a single pore. The mechanism of the events in such a pore can be described by three key equations (Meares & Page, 1972). These equations express (per unit area) local salt flux J_s, electric current i and volume flow $\bar{v}$ each averaged over the pore cross-section. They are

$$J_s = -\frac{1}{v}(v_1 D_1 + v_2 D_2)\frac{d\rho_s}{dx} - \frac{v_1 v_2}{v} F \rho_s (u_1 - u_2)\frac{d\psi}{dx} + \rho_s \bar{v}, \tag{1}$$

$$i = -\frac{v_1 v_2}{M_s} F(D_1 - D_2)\frac{d\rho_s}{dx} - \frac{v_1 v_2}{v} F^2 \rho_s (v_2 u_1 + v_1 u_2)\frac{d\psi}{dx}, \tag{2}$$

$$\bar{v} = -\frac{a^2}{8\eta}\frac{dP}{dx} + \frac{\sigma}{\kappa\eta}\frac{d\psi}{dx}. \tag{3}$$

J_s is related to the cation and anion fluxes J_1 and J_2, respectively, by

$$J_s = \frac{M_s}{v}\left(\frac{J_1}{M_1} + \frac{J_2}{M_2}\right) \tag{4}$$

and to the electric current i by

$$i = e_1 J_1 + e_2 J_2. \tag{5}$$

In these equations subscripts 1 and 2 indicate cations and anions, respectively, and subscript s refers to the electrically neutral salt. ρ_s is the specific salt concentration, ψ the electric potential and x the axial coordinate along the pore. D_i and u_i are ionic diffusion and mobility coefficients, respectively.

e_i represents the electrical charge per unit mass of ions i, and v_i is the stoichiometric coefficient of i in the salt. v is the sum of v_1 and v_2. F is the Faraday constant. M_i and M_s are the molecular weights of ions and salt, respectively. η is the coefficient of shear viscosity of the solution, a the radius of the pore and σ the surface charge per unit area on the pore wall. P represents the hydrostatic pressure and κ the Debye-Hückel reciprocal length which is defined by

$$\kappa = 4\pi F^2 v_1 v_2 \rho_s / \varepsilon RTM_s$$

in the notation used here. R is the gas constant, T the absolute temperature and ε the bulk dielectric constant.

Eqs. (1) and (2) are written here in the form of combinations of the Nernst-Planck flux equations with an additional term to deal with the effects of convection. Previously, they were derived by using the methods of irreversible thermodynamics. The coupling of water and ion fluxes in the barycentric reference frame and perturbations in the ion fluxes caused by the electrical double layer at the pore wall were neglected. Within the limitations of these assumptions the equations correctly express coupling between the water and ion fluxes with the membrane taken as stationary reference frame.

Eq. (3) is a solution of the Navier-Stokes equation with the pressure dependent part of the volume flow described in terms of the Hagen-Poiseuille law and the electrical part by using the Gouy-Chapman theory to calculate electro-osmosis. The simple form of Eq. (3) results from the cylindrical conformation of the pore. The pore length was assumed to be much greater than the pore diameter so that end effects could be neglected. In this equation the volume flow was averaged across the pore cross-section by using the relation

$$\bar{v} = \int_0^a 2\pi r v dr \Big/ \int_0^a 2\pi r dr \tag{6}$$

where v is the local stream line velocity and r the radial coordinate in the pore.

To express the behavior of the membrane in its cell it is necessary to integrate Eqs. (1)–(3) along the length of the pore, by introducing the limits

$$\begin{aligned} &\rho_s = \rho_{\mathrm{I}}^m, P = P_{\mathrm{I}}, \quad \psi = \psi_{\mathrm{I}} \quad \text{at} \quad x = 0 \\ &\rho_s = \rho_{\mathrm{II}}^m, P = P_{\mathrm{II}}, \quad \psi = \psi_{\mathrm{II}} \quad \text{at} \quad x = l \end{aligned} \tag{7}$$

and the stationary state conditions

$$dJ_s/dx = di/dx = d\bar{v}/dx = 0. \tag{8}$$

The concentrations ρ_{I}^m and ρ_{II}^m represent the salt concentrations at the ends of the pore. They are different from the bulk concentrations owing to the presence of poorly stirred layers of solution adjacent to each membrane face. They may be related to the bulk concentrations by using the Nernst stagnant diffusion layer hypothesis. The appropriate relations were given earlier (Meares & Page, 1972).

The surface charge on the pore walls resulted from the adsorption of ions and it was found that it could be related to the concentration of the electrolyte by

$$\sigma = K\rho_s^{1/3} \tag{9}$$

where K is a constant independent of concentration. The integral pore flux densities may be related to the flows per unit area of membrane by using

$$(J)_{\text{membrane}} = \pi a^2 N_m (J)_{\text{pore}} \tag{10}$$

where N_m represents the number of pores per unit area of membrane. The current density and volume flow relating to unit area of membrane will be indicated by I_m and V_m.

The integrations lead to final equations which are complicated (Meares & Page, 1972) and it will be simpler here to discuss their properties by using numerical solutions. For the purpose of the following discussion, the convention is adopted that positive fluxes flow from the dilute to the concentrated side of the membrane; i.e., from compartment I to compartment II and that

$$\Delta P = P_{\mathrm{I}} - P_{\mathrm{II}}, \tag{11}$$

$$\Delta\psi = \psi_{\mathrm{I}} - \psi_{\mathrm{II}}. \tag{12}$$

$\Delta\psi_T$ will indicate the potential difference measured by the probes B. This includes the potential drop across the solutions between the probes and the membrane as well as $\Delta\psi$. The membrane resistance R_m is defined by $\Delta\psi/I_m$.

Bi-stable Stationary-State Phenomena

In Fig. 2 it was shown how the analogue switched from one stable stationary state to another in response to changes in current density at a constant pressure differential. The reason for the transitions lies in the dependence of electro-osmosis on concentration and membrane potential and in the dependence of the concentration profile along each pore upon the net volume flow.

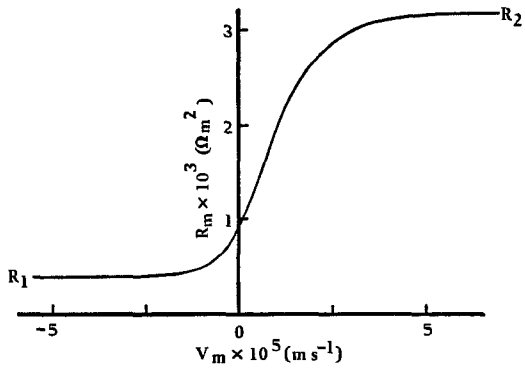

Fig. 3. Membrane resistance *vs.* volume flow calculated for membrane B when separating solutions of 0.1 and 0.01 mol dm^{-3} NaCl

An expression for this profile is obtained by integrating Eqs. (1) and (2). It has the form

$$\rho_s(x) = A \exp(\bar{v}x/D_s) + B \tag{13}$$

where

$$D_s = (v_2 u_1 D_2 + v_1 u_2 D_1)/(v_2 u_1 + v_1 u_2). \tag{14}$$

Here A and B are constants for the membrane and the pair of electrolyte concentrations. The electrical resistance of the membrane is determined by the concentration profile. Thus, it is found that the resistance is related to the volume flow by the function which is plotted in Fig. 3.

The integrated form of the volume flow Eq. (3) contains three terms. The first describes the pressure-driven flow, the second and third relate the electro-osmotic flow to the electric current. Concentration dependence enters these terms on two counts. The electro-osmotic permeability is a function of the surface charge density and the double-layer thickness at the pore wall. Both these parameters are concentration dependent. Furthermore, the electro-osmosis is driven by the potential gradient which, through its proportionality to the resistance, bears a concentration dependent relation to the current.

In consequence, the relation between the net volume flow and electric current is far from linear as is shown in Fig. 4. It will be noted that the relationship becomes more markedly nonlinear the larger the pressure differential. In a galvanostatic experiment the region between the turning points is inaccessible and the system must follow the paths indicated by the dotted lines, shown in Fig. 4 for a pressure differential of -687 Pa. On this diagram the vertical turning points indicate the positions of the transition currents I_1 and I_2 which appear on Fig. 2.

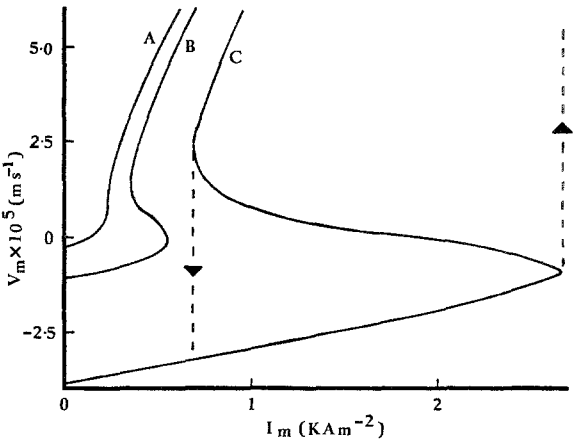

Fig. 4. Volume flow *vs.* current density calculated for membrane B when separating solutions of 0.1 and 0.01 mol dm^{-3} NaCl. Pressure differentials are: curve *A*, −45 Pa; curve *B*, −196 Pa; and curve *C*, −687 Pa. The dotted lines indicate paths of transitions under galvanostatic conditions when $\Delta P = -687$ Pa

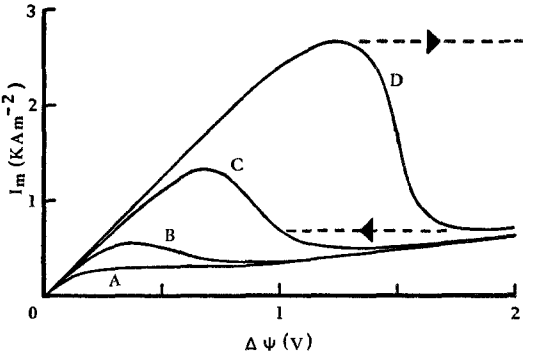

Fig. 5. Current density *vs.* membrane potential calculated for membrane B when separating solutions of 0.1 and 0.01 mol dm^{-3} NaCl. Pressure differentials are: curve *A*, −45 Pa; curve *B*, −196 Pa; curve *C*, −392 Pa; and curve *D*, −687 Pa. The dotted lines for $\Delta P = -687$ Pa indicate transitions under galvanostatic conditions

Fig. 4 reveals the points of transition in any flip-flop cycle, while for the same cycle Fig. 3 indicates the nature of the stationary states which are represented by R_1 and R_2. Fig. 5 conveniently summarizes these properties by combining Figs. 3 and 4 to give the current-voltage relationship directly. Fig. 5 demonstrates the so-called dynatron characteristics of the system. In galvanostatic systems, the region between the maximum and minimum of each curve is inaccessible and the system must follow a course such as indicated by the dotted line for the highest pressure. Once an allowance has been made for the resistance of the solutions between the membrane faces and the probe electrodes, Fig. 5 permits prediction of current-voltage curves, such as are shown in Fig. 2, for comparison with experiment.

Factors Affecting Bi-stability

The considerations in the previous section show that the operation of the analogue may be summarized in the form of a parametric feedback loop. This type of loop has been discussed by Katchalsky and Spangler (1968). It is shown in Fig. 6. The operation of the loop underlies the regenerative behavior to be discussed in a later section of this paper.

Factors that either increase the hydrodynamic permeability or decrease the electro-osmotic permeability of the membrane have two effects. They increase the sensitivity of the system to pressure changes and increase the transition currents I_1 and I_2. This is clearly demonstrated by Figs. 7 and 8. These figures compare the observed I_1 and I_2 at different pressures for several membranes separating the same pair of sodium chloride solutions. The properties of the membranes are listed in Table 1. The hydrodynamic permeability of each membrane is indicated by L_p. It increases and the electro-osmotic permeability, which is indicated by K, decreases in the sequence A to C. It will be seen that I_1, I_2 and the slopes $dI/d\Delta P$ increase in the same sequence and in conformity with the prediction above.

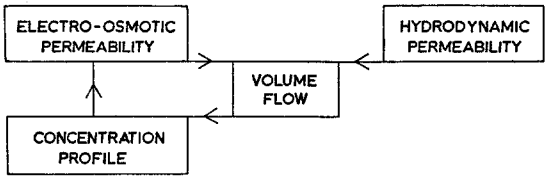

Fig. 6. Factors affecting the volume flow

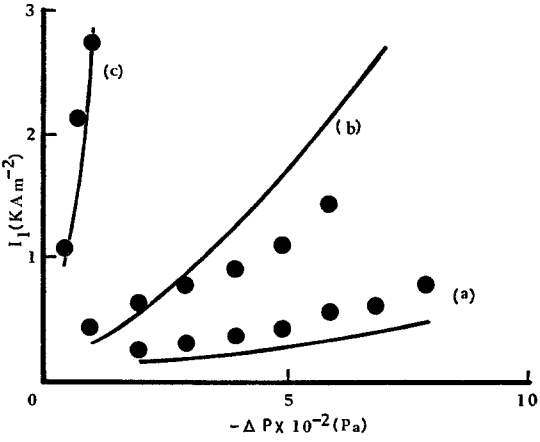

Fig. 7. Flip-over currents *vs.* pressure differentials for membrane A, curve (*a*); membrane B, curve (*b*); and membrane C, curve (*c*). Each membrane separates solutions of 0.1 and 0.01 mol dm^{-3} NaCl. Curves indicate calculated results and the points are observed results

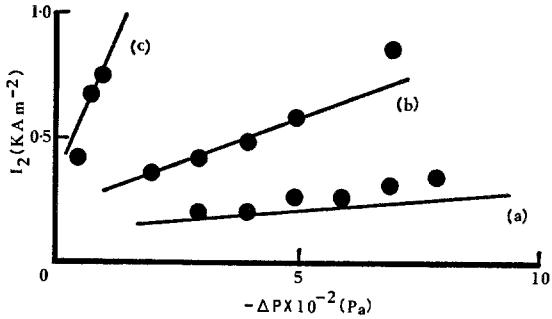

Fig. 8. Flop-over currents *vs.* pressure differentials for membrane A, curve (*a*); membrane B, curve (*b*); and membrane C, curve (*c*). Each membrane separates solutions of 0.1 and 0.01 mol dm^{-3} NaCl. Curves indicate calculated results and the points are observed results

Table 1. Membrane properties

Membrane	a* (μm)	$N_m \times 10^{-10}$ (pore m^{-2})	l (μm)	$L_p \times 10^8$ (m^3 N^{-1} sec^{-1})	K (m cm^{-1} Kg$^{-1/3}$)
A	0.221	27	12.0	2.35	−9.84
B	0.422	5.0	12.4	5.62	−5.21
C	0.758	2.3	9.15	36.2	−4.35
D	0.727	2.3	9.15	30.8	−3.67

* Calculated from N_m, l, and L_p by using Eq. (14). At all membranes, the thickness of the unstirred solution layers δ was estimated as being 106 μm.

L_p is given by

$$L_p = \pi a^4 N_m / 8\eta l \tag{15}$$

where l is the membrane thickness. It can be seen that L_p is very sensitive to the pore radius a. Changes in L_p and K have opposing effects on I_1 and I_2. Fig. 9 compares the experimental results and theoretical predictions for membranes C and D. L_p increases by 17.6% and K increases by 18.7% from membrane D to membrane C (*see* Table 1). It is seen that observation and theory agree that in I_1 the changes caused by the increase in K are just offset by the slightly smaller increase in L_p while I_2 is considerably larger in membrane D than in C at the same pressure differential.

In this paper consideration is restricted to 0.10 and 0.01 mol dm^{-3} NaCl solutions. It may be mentioned however that changes in the pairs of concentrations and in the type of electrolyte also affect the electro-osmotic permeability. Such changes have been systematically analyzed (Meares & Page, 1972) and have been found to conform to the principles presented above.

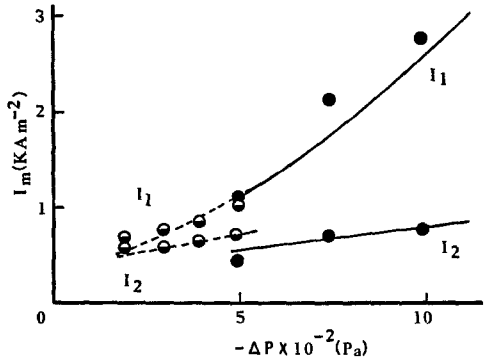

Fig. 9. Flip-flop currents *vs.* pressure differentials for membranes separating solutions of 0.1 and 0.01 mol dm^{-3} NaCl. Full lines indicate calculated results for membrane C; dotted lines calculated results for membrane D. Points represent observed results: • membrane C; ∘ membrane D

Excitatory Response to Stimuli

The biological analogue properties of this system will be discussed in terms of the following concepts: the high concentration side of the membrane, compartment II, will be considered to represent the interior of a biological cell. The high resistance state will be considered as the resting state, and the low resistance state as an excited state. Factors causing transitions between these states are regarded as analogous to stimuli inducing excitation.

Current-Induced Stimulation

Stimulation by changes in the electric current may be understood in terms of the relation shown in Fig. 2. The resting state corresponds to a current density greater than I_1 while the pressure is kept constant. Stimulation is achieved by reducing the current density below I_2. The system follows the arrows in Fig. 2 and undergoes a transition at I_2. The membrane resistance then falls with a consequent fall in the membrane potential. This is analogous to depolarization. Simultaneously, the volume flow reverses direction from positive, i.e. inward, to a negative, i.e. outward flow.

On removing the stimulus, the current density is restored to its original value and the system returns to the resting state at the moment when I_1 is reached. The return to the resting state is by a path different from that followed during excitation, i.e. $I_1 > I_2$, and the system therefore shows hysteresis.

Pressure-Induced Stimulation

Excitation may be produced by raising the pressure on the concentrated solution, i.e. the cell interior. This is shown in Figs. 10 and 11 which have been calculated by using the data for membrane A. In Fig. 10 two of the family of dynatron curves obtained at different set pressure differentials are plotted. These have been selected so that the flop-over current I_2 of the high pressure curve ($\Delta P''$) is the same as the flip-over current I_1 of the

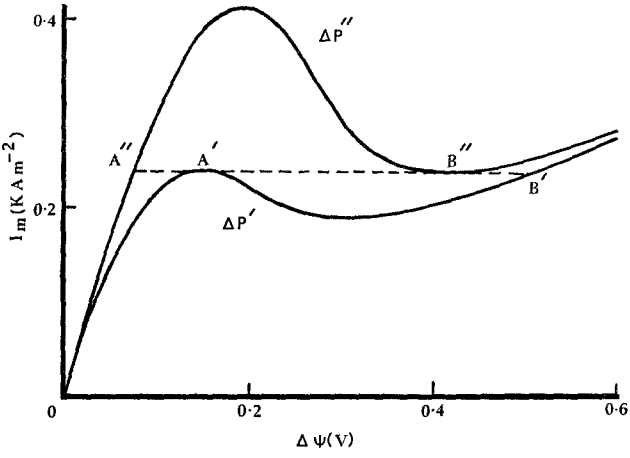

Fig. 10. Current density *vs.* membrane potential calculated for membrane A when separating solutions of 0.1 and 0.01 mol dm^{-3} NaCl. The dotted line represents the path of transitions for pressure stimulation for a constant current density of 0.24 kA m^{-2}. $\Delta P' = -392$ Pa, $\Delta P'' = -686$ Pa

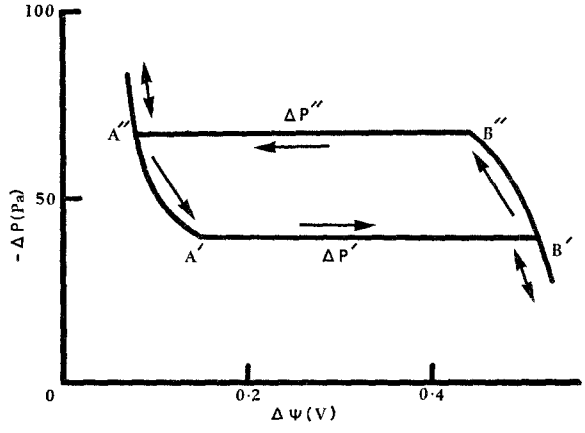

Fig. 11. Pressure differential *vs.* membrane potential calculated for membrane A when separating solutions of 0.1 and 0.01 mol dm^{-3} NaCl and with a constant current density of 0.24 kA m^{-2}. The arrows indicate the path of transitions for pressure stimulation

low pressure curve ($\Delta P'$). Fig. 11 indicates the relationship between ΔP and $\Delta\psi$ at this current density. It will be seen that the ΔP *vs.* $\Delta\psi$ relationship is single valued except in the region between $\Delta P'$ and $\Delta P''$.

Fig. 11 shows that at this constant current density the system is in the resting state for pressures less than $\Delta P'$. On increasing the pressure differential the system moves along the line $B'B''$ until the pressure $\Delta P''$ is reached. Excitation now occurs corresponding to the transition from B'' to A''. The system remains in the excited state until the pressure is lowered to $\Delta P'$ at which point the reverse transition takes place. Under galvanostatic conditions, the system can follow only the routes indicated by the arrows in Fig. 11 and therefore shows hysteresis.

Stimulation Induced by Mechanical Deformation

It is possible that permeability changes caused by mechanical deformation of a membrane may lie behind the action of a number of natural mechano-receptors (Loewenstein, 1956, 1971; Teorell, 1966, 1971). In a previous section, the role of the hydrodynamic permeability was discussed. It can be inferred from Eq. (15) that the hydrodynamic permeability coefficient L_p is extremely sensitive to a change in the pore radius. In the system considered here the tensile strength of the Nuclepore membranes precluded any significant changes in pore radius arising from stress. However, a series of Nuclepore membranes was studied in which the pore radii differed. The consequent differences in properties between these membranes were successfully described by the theory. It is interesting, therefore, to use the theory to examine what would be the effect of varying the pore radius when all other membrane properties were held constant. This is equivalent to studying the effects of a radial tension upon an extensible membrane with a pore structure similar to that of the Nuclepore.

Figs. 12 and 13 represent the behavior predicted for a membrane with properties identical to those of membrane A in Table 1 except that it is extensible. In the calculation the pressure differential was kept constant. Fig. 12 shows two of a family of dynatron curves produced by varying the pore radius under these conditions. They have been chosen so that the flop-over current corresponding to the larger pore radius a'' is the same as that of the flip-over current for the smaller pore radius a'. Fig. 13 shows the relationship between pore radius a and $\Delta\psi$ at this current density. Under conditions of constant current and pressure the a *vs.* $\Delta\psi$ curve shows hysteresis. At radii less than a' the system is in the resting state. On increasing the pore radius, excitation is predicted at the point B'' corresponding to

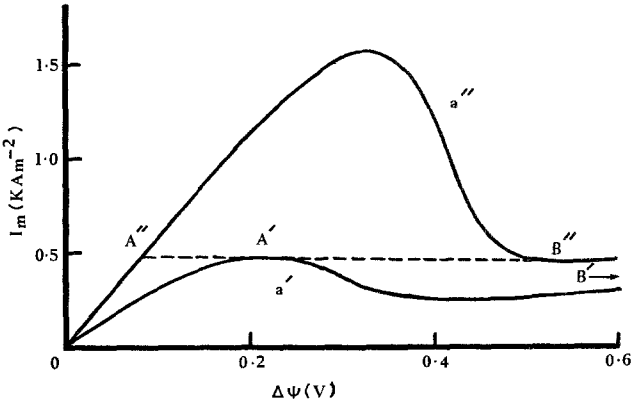

Fig. 12. Current density *vs.* membrane potential calculated for an extensible membrane when separating solutions of 0.1 and 0.01 mol dm^{-3} NaCl. The dotted line represents transitions for a stimulation by stretching under a constant pressure of −785 Pa and a constant current of 0.48 kA m^{-2}. $a'=0.22$ μm; $a''=0.28$ μm

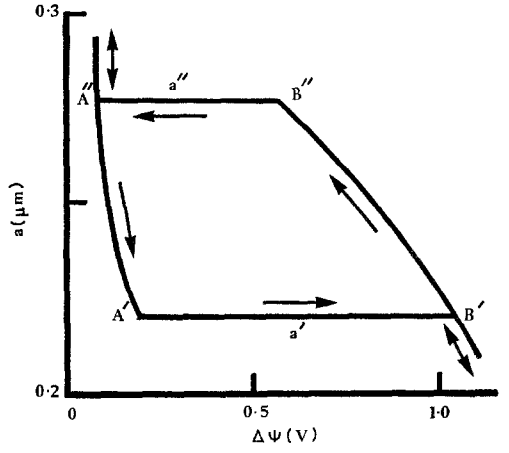

Fig. 13. Pore radius *vs.* membrane potential calculated for an extensible membrane when separating solutions of 0.1 and 0.01 mol dm^{-3} NaCl at a constant pressure of −785 Pa and a constant current of 0.48 kA m^{-2}. The arrows indicate the path of transitions for stimulation by stretching

radius a''. The system now must remain in the excited state until the radius is decreased again to a'. $A'B'$ marks the transition back to the resting state and $B'B''A''A'$ is the predicted hysteresis loop.

This particular example shows that a change in pore radius from 0.22 to 0.28 μm would be sufficient to induce the transition phenomenon. Thus, a 15% increase in pore radius would be sufficient to cause an excitation. As pointed out by Burton (1970), provided the Poisson ratio of the membrane material is not too low, the pores act as foci of stress and a small

increase in the membrane diameter will cause a proportionately much greater increase in pore diameter. It is possible that such a phenomenon may be of importance in the more extensible materials frequently associated with natural membranes.

Regenerative Behavior

This paper has been restricted so far to the stationary-state properties of the analogue system. When the pressure differential is not kept constant it is possible to obtain regenerative phenomena including undamped oscillations. Fig. 14 illustrates a series of oscillations of pressure and potential obtained using a 1-μm pore diameter membrane in a cell equivalent to the open-topped conpartment cell originally used by Teorell (1959*a*). Oscillatory phenomena would be expected owing to the hysteresis shown by the system. Wave trains of the form shown in Fig. 14 were generated at current densities greater than a critical value characteristic of the membrane and electrolyte solutions. Below this critical value of the current the oscillations were damped. Fig. 15 illustrates a sequence of responses in potential obtained using a membrane with 0.8-μm diameter pores and a series of different current densities. The critical current density for stable oscillations in this case was in the region of 19 kA m^{-2}.

To explore the system more effectively as a possible biological analogue it would be necessary to modify the open-topped cell by inserting an over-

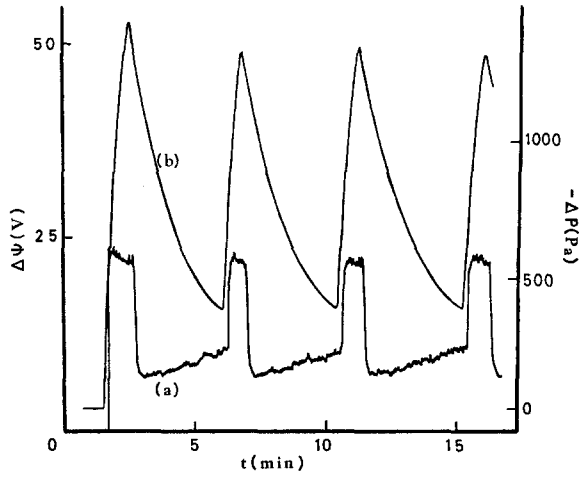

Fig. 14. Undamped oscillations across a membrane with 1-μm pores. Variations in the total potential are recorded by trace (*a*), and variations in the pressure differential by trace (*b*). Both are plotted as functions of time. The membrane separated solutions of NaCl at 0.1 and 0.01 mol dm^{-3} and the cell was fitted with tubes 5 mm in diameter. A current density of 1.82 kA m^{-2} was used

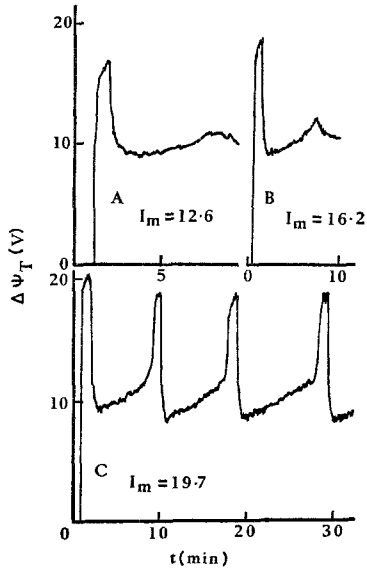

Fig. 15. The effect of increasing current density. The variations of total potential with respect to time are shown for several current densities using a membrane with 0.8-μm pores separating solutions of NaCl at 0.1 and 0.01 mol dm^{-3}. The cell was fitted with tubes 3 mm in diameter. The critical current density lies between 16.2 and 19.7 kA m^{-2}

flow at the top of the cell which interconnected compartments I and II (Teorell, 1966). The consequence of this modification would be that the resting state of the membrane in the apparatus would now correspond with the resting state defined in the previous section. This system would respond to the three stimuli discussed above by a change in the membrane state. When the level of the solution in compartment II fell below the level of the overflow, the system would correspond to that examined by Meares and Page (1972). The analogue would then show the time-dependent phenomena described by them. On removing the stimulus, the level of the solution would rise in compartment II until checked by the overflow and the system would resume its resting state.

Scope and Limitation of the Analogue

When the analogue is fitted with an overflow device interconnecting the cell compartments, stimulation produces an immediate lowering of the membrane potential. The rise in membrane conductivity results from an outflux of concentrated electrolyte. As a result, the pressure falls in the

concentrated compartment, i.e. the compartment which represents the inside of the cell. The initial depolarization of the membrane is therefore associated with a fall in "turgor". If the source of the stimulus is not removed, a train of oscillations follows. On removing the stimulus, the system returns to its resting state leading to a full recovery of turgor and resting potential. Such stimulation may be produced electrically or mechanically.

These events may be compared phenomenologically to the action potentials observed in a variety of living tissues. The action potential in *Chara australis* is closely accompanied by an outwardly directed volume flow and a fall in turgor. This is followed by a recovery phase in which the cell regains its resting volume and turgor (Barry, 1970). Similar results have been reported also for other species of giant algae. A similar sequence of events has been observed during the excitation of the motor cells of species of *Mimosa* and *Dionaea* (Sibaoka, 1969). Excitation of giant algae (Teorell, 1961) and of *Dionaea* and *Aldrovanda* (Sibaoka, 1969) may be produced by electrical stimuli as well as by mechanical stimuli.

The recent observations of Benolken and Jacobson (1970) on the indented cells forming part of the sensory hairs of *Dionaea muscipula* (Venus's-fly-trap) are of particular interest in the present context. According to these authors, the mechanical deformation of a single sensory hair is transduced into electrical signals by the indented cells. A graded response is obtained by subthreshold stimuli and an action potential is produced by stimuli above the threshold. In their analysis of the behavior of these cells they concluded that in the resting state the cell walls adjacent to the podium and lever tissues had similar permeabilities. On stimulation, however, the electrical conductivity of the cell walls adjacent to the podium of the hair appeared to increase by at least 100-fold while that of the cell walls adjacent to the hair lever tissues rose by only threefold.

The relevance of the membrane analogue to these observations appears when it is appreciated that the lever tissue is of a woody nature and more resistant to mechanical deformation than the softer podium tissue. The cell walls adjacent to the lever are therefore less likely to be deformed during a mechanical stimulus than those adjacent to the podium. It was pointed out in the previous section that under these circumstances the behavior of the analogue would predict a flip-flop transition and a sharp increase in conductivity of the cell wall adjacent to the podium but not in the area adjacent to the lever.

Excitation produced by mechanical deformation is of special importance in the case of animal tissues. A wide variety of animal mechano-receptors appear to depend upon a stretch-induced excitation of a transducer mem-

brane for their action (Loewenstein, 1971). The Pacinian corpuscle consists of a bulb-shaped lamella structure surrounding the unmyelinated terminal of a dendrite. The transducer action of the corpuscle appears to be located in the dendrite membrane. Forces that extend this membrane elicit an excitatory response marked by a sharp increase in the membrane conductivity. Axially symmetric forces, on the other hand, produce no response (Loewenstein, 1965). This behavior is consistent with the analysis of mechanically induced stimulation presented earlier. The relation between the analogue and the behavior of animal tissues is less clear-cut than in the case of plant tissues, however. In the latter, clearly defined hydrostatic pressure differentials exist across the excitable tissues. Hydrostatic pressure gradients are less obvious in animal tissues, although it is possible that they occur at a local level (Teorell, 1971). The time sequence of the action potential generated by the analogue is of the same order as found in plants, but a good deal slower than that found in animal tissues. It is possible to envisage conditions which would produce faster responses from the analogue, but the shortest period observed so far with the present system is of the order of one minute.

This paper has concentrated on the physico-chemical mechanisms underlying the excitation processes found in Teorell's membrane oscillator. For this purpose, it has been necessary to restrict attention to the simplest experimental configuration of the analogue. This basic configuration may be used to build up more-complex models which mimic more accurately the behavior of biological organs (Teorell, 1971). All such models ultimately rely upon the three basic excitatory mechanisms considered in this paper.

Two important points arise from the present study. The first emphasizes the potential importance of nonlinear force-flux coupling in the excitation process. Coupling of this type is frequently neglected when the translocation properties of natural tissues are analyzed. The properties of this analogue arise directly from its nonlinearity and a similar situation would be expected in natural tissues undergoing the excitation process. The second point indicates the possible importance of electro-osmotic coupling between ion and water fluxes in excitable biological tissues, in particular in plants where the cell walls might contribute to the phenomena. Lack of knowledge concerning the microscopic properties of biological tissues makes it impossible to draw definite conclusions on this matter.

The present membrane cannot be regarded as a specific model of any real biological tissue. However, if its pores were reduced to the dimensions attributed to biological pores and the pore density likewise increased then, provided some fixed charge was associated with the membrane matrix,

phenomena similar to those discussed in this paper should occur. A theoretical treatment of the behavior expected in these circiumstances would involve two extra considerations. The space charge would extend almost uniformly across the pores instead of being concentrated into an electrical double layer close to their walls. If the thickness of the membrane were greatly reduced then, depending upon the ratio of length to radius, end effects in the pores might also have to be taken into account.

Structurally, this membrane analogue is far too simple to account for the complete behavior of any particular biological membrane. It neglects the selective permeability found in living tissues (Barry, 1970) and it does not involve the metabolic origin of the electrical current necessary for the operation of a living system. The purpose of this paper has been to indicate the consequence of the detailed interplay between ion and water fluxes created by gradients of hydrostatic pressure, concentration and electrical potential in a membrane of clearly defined structure. It has indicated also the importance of nonlinear force-flux coupling in the excitability phenomena. Many of the features associated with excitability can be reproduced by an electro-osmotic mechanism.

The authors wish to acknowledge the valuable help granted to them by Professor U.F. Franck and his co-workers at the Technische Hochschule, Aachen, during the early stages of this project.

References

Barry, P.H. 1970. Volume flows and pressure changes during an action potential in cells of *Chara australis*. II. Theoretical considerations. *J. Membrane Biol.* **3**:335.

Benolken, R.M., Jacobson, S.L. 1970. Response properties of a sensory hair excised from Venus's-flytrap. *J. Gen. Physiol.* **56**:64.

Burton, A.C. 1970. The stretching of 'pores' in a membrane. *In*: Permeability and Function of Biological Membranes. L. Bolis, editor. p. 1. North Holland Publishing Co., Amsterdam.

Drouin, H. 1969. Experimente mit dem Teorellschem Membran oszillator. *Ber. Bunsenges. Phys. Chem.* **73**:223.

Franck, U.F. 1963. Über das elektrochemische Verhalten von porosen ionenaustauschermembranen. *Ber. Bunsenges. Phys. Chem.* **67**:657.

Jancke, H. 1962. Das electrochemische Verhalten von porosen ionenaustauschermembranen. Dr. rev. nat. Dissertation, Darmstadt.

Katchalsky, A., Spangler, R. 1968. Dynamics of membrane processes. *Quart. Rev. Biophys.* **1**:128.

Kobatake, Y., Fujita, O. 1964. Flows through charged membranes. I. Flip-flop current versus voltage relation. *J. Chem. Phys.* **40**:2212.

Loewenstein, W.R. 1956. Excitation and changes in adaptation by stretch of mechanoreceptors. *J. Physiol.* **133**:588.

Loewenstein, W.R. 1965. Facets of a transducer process. *Cold Spr. Harb. Symp. Quant. Biol.* **30**:29.

Loewenstein, W.R. 1971. Mechano-electric transduction in the Pacinian corpuscle. Initiation of sensory impulses in mechanoreceptors. *In*: Handbook of Sensory Physiology. W.R. Loewenstein, editor. Vol. 1., Ch. 9. Springer-Verlag, Berlin.

Meares, P., Page, K.R. 1972. Rapid force-flux transitions in highly porous membranes. *Phil. Trans., Ser. A.* **272**:1.

Mikulecky, D.C., Caplan, S.R. 1966. The choice of reference frame in the treatment of membrane transport by non-equilibrium thermodynamics. *J. Phys. Chem.* **70**:3049.

Sibaoka, T. 1969. Physiology of rapid movements in higher plants. *Annu. Rev. Pl. Physiol.* **20**:165.

Teorell, T. 1959*a*. Electro-kinetic membrane processes in relation to properties of excitable tissues. I. Experiments on oscillatory transport phenomena in artificial membranes. *J. Gen. Physiol.* **42**:831.

Teorell, T. 1959*b*. Electro-kinetic membrane processes in relation to properties of excitable tissues. II. Some theoretical considerations. *J. Gen. Physiol.* **42**:847.

Teorell, T. 1961. An analysis of the current-voltage relationships in excitable *Nitella* cells. *Acta Physiol. Scand.* **53**:1.

Teorell, T. 1966. Electro-kinetic considerations of mechanoelectric transduction. *Ann. N. Y. Acad. Sci.* **137**:950.

Teorell, T. 1971. A biophysical analysis of mechano-electrical transduction. *In*: Handbook of Sensory Physiology. W.R. Loewenstein, editor. Vol. 1, Ch. 10. Springer-Verlag, Berlin.